NASA Contractor Report 186024

Lee Waves: Benign and Malignant

M.G. Wurtele, A. Datta, and R.D. Sharman

June 1993

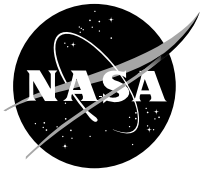

National Aeronautics and
Space Administration

NASA Contractor Report 186024

Lee Waves: Benign and Malignant

M.G. Wurtele, A. Datta, and R.D. Sharman
Department of Atmospheric Sciences
University of California
Los Angeles, CA 90024-1565

Prepared for
Dryden Flight Research Facility
Edwards, California

1993

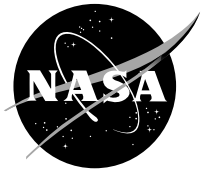

National Aeronautics and
Space Administration

Dryden Flight Research Facility
Edwards, California 93523-0273

CONTENTS

ABSTRACT

The flow of an incompressible fluid over an obstacle will produce an oscillation in which buoyancy is the restoring force, called a gravity wave. For disturbances of this scale, the atmosphere may be treated as dynamically incompressible, even though there exists a mean static upward density gradient. Even in the linear approximation—i.e., for small disturbances—this model explains a great many of the flow phenomena observed in the lee of mountains. However, nonlinearities do arise importantly, in three ways: (i) through amplification due to the decrease of mean density with height; (ii) through the large (scaled) size of the obstacle, such as a mountain range; and (iii) from dynamically singular levels in the fluid field. These effects produce a complicated array of phenomena—large departure of the streamlines from their equilibrium levels, high winds, generation of small scales, turbulence, etc.—that present hazards to aircraft and to lee surface areas. The nonlinear disturbances also interact with the larger-scale flow in such a manner as to impact global weather forecasts and the climatological momentum balance. If there is no dynamic barrier, these waves can penetrate vertically into the middle atmosphere (30–100 km), where recent observations show them to be of a length scale that must involve the coriolis force in any modeling. At these altitudes, the amplitude of the waves is very large, and the phenomena associated with these wave dynamics are being studied with a view to their potential impact on high performance aircraft, including the projected National Aerospace Plane (NASP). The presentation herein will show the results of analysis and of state-of-the-art numerical simulations, validated where possible by observational data, and illustrated with photographs from nature.

1. INTRODUCTION

A **gravity wave**—the term "wave" is used loosely—is a disturbance in a fluid propagated by the force of buoyancy. The simplest realization, at least in its linear formulation, is the wave on a density discontinuity, such as air-water, that can propagate in two dimensions. In the atmosphere, or in the thermocline beneath the surface of the oceans, the density varies continuously along the vertical—the fluid is then said to be stratified—and in this environment a disturbance can propagate in three dimensions.

When a density-stratified fluid flows over a solid obstacle, the disturbance thus produced is called a lee wave, or when the obstacle is a mountain range, a mountain wave. At this point, at the risk of belaboring the obvious, we may distinguish a number of flows that are familiar to those acquainted with fluid dynamics.

(i) Two-dimensional homogeneous, incompressible, inviscid flow over solid boundaries—potential flow—solved by the methods of the theory of functions of a complex variable.
(ii) Homogeneous, incompressible, viscous flow over solid boundaries, for Reynolds numbers from small to large enough to produce turbulence.
(iii) Compressible flow over solid boundaries, notably airfoils, for Mach numbers from small to large enough to produce shock waves.

The gravity-lee-wave problem for the atmosphere is different from all of these. In the first place, the planetary boundary layer of the atmosphere in contact with the earth is characterized by a Reynolds number of the order of 10^7, and is always and everywhere turbulent. On the scale of interest to us in this discussion, viscosity plays no role. In the second place, the buoyancy of the fluid provides a mechanism for the horizontal and vertical propagation of any disturbance away from the obstacle, so that the concern of lee-wave researchers has traditionally been in this purely inviscid phenomenon, on a scale far larger than that of the obstacle itself. The inviscid results have had remarkable success in predicting certain phenomena close to the surface. Currently modelers are attempting to introduce a parameterized turbulent boundary layer; however, a complete theory for close-in and far-field behavior using such a model has not yet been demonstrated.

The most familiar realization of a gravity lee wave is the so-called ship, or bow, wave on a water surface. The counterpart for a continuously stratified fluid—say, atmospheric flow over a mountain—has strong similarities to, and differences from, the ship wave, as brought out by Wurtele (1957) and Sharman and Wurtele (1983). In fact, in the first of these articles it is shown that the simplest atmospheric case has an asymptotic analytic solution. Figure 1 reproduces a satellite image of an atmospheric ship wave, where the visualization is achieved by cloud condensation in the crests of the wave. Figure 2 is an example of the simulation of this phenomenon at two vertical levels in the atmosphere. In the oceans, the passage of a submarine through the thermocline sets up a lee-wave pattern that has been suggested as a possible means of its detection from satellite by synthetic aperture radar. An interesting feature of the surface ship wave is the characteristic transient—visualized in Figure 3 by the clusters of short waves at the leading edge (that is, toward the right in the figure)—a configuration never present in the transient development of atmospheric lee waves.

When a lee wave achieves a steady state—usually predictable from linear theory—we have called it **benign**. The atmospheric ship wave is a prototypical instance of such a benign wave. However, through one of a number of dynamic mechanisms that will be discussed later, the disturbance may fail to become steady, and/or may generate a cascade of energy into higher wave numbers, finally breaking down into turbulence, called **clear air turbulence**. These phenomena we have called **malignant**, a term not entirely facetious, since much damage to aircraft and to lee-side surface structures has been attributed to them.

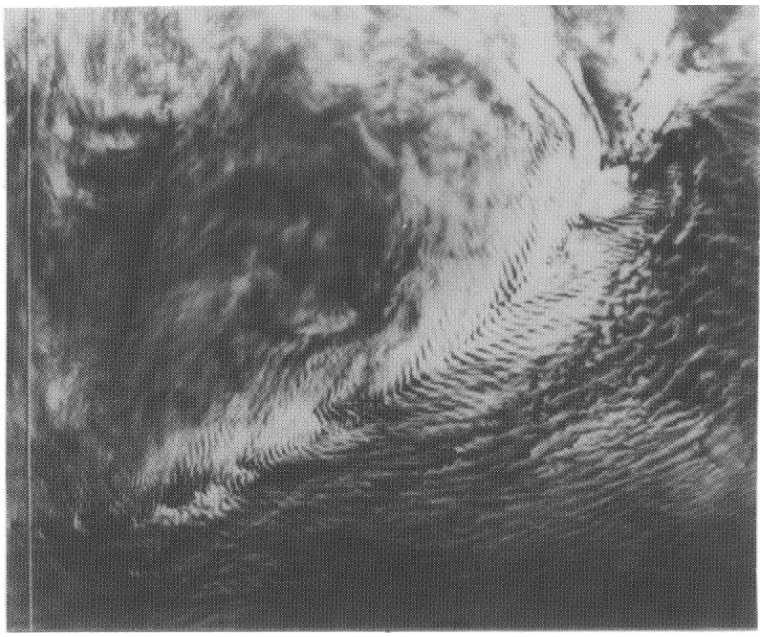

Figure 1. Atmospheric ship wave pattern in the vicinity of the Aleutian Island chain. Note that these waves are dominantly of the transverse type. Time and date of photograph unknown. (Sharman and Wurtele, 1983)

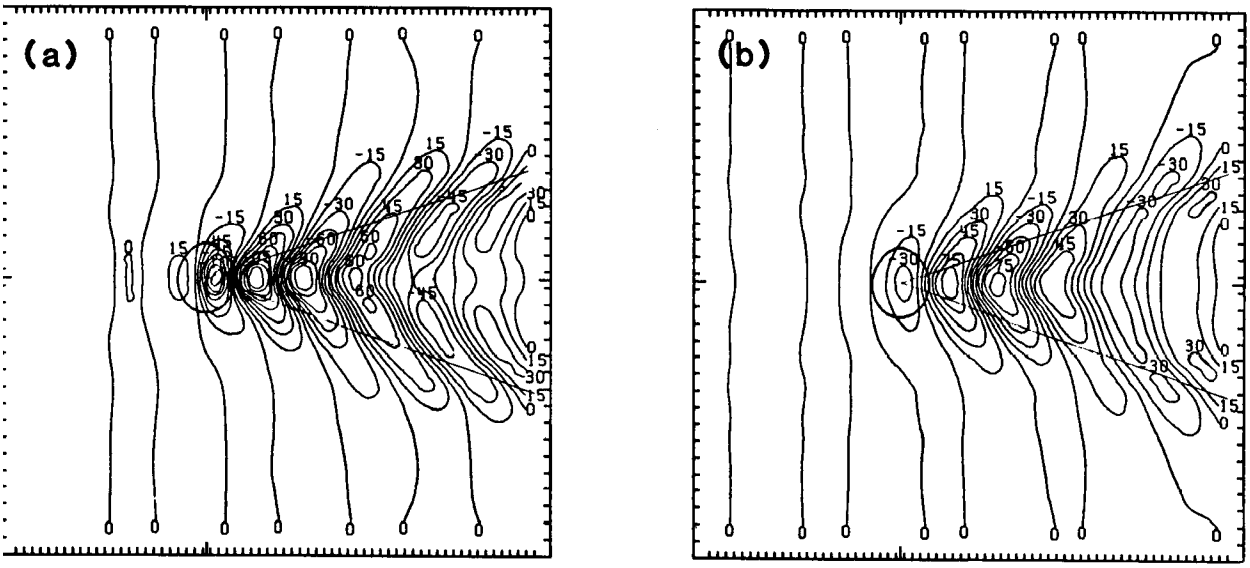

Figure 2. Contours of vertical velocity at (a) 2 km (b) 4 km elevation after 800 time steps (200 min) for three dimensional $R = 5.6$ (R is the square root of the Richardson number at $z = 0$) simulation over a Gaussian obstacle. The contour interval is 15 cm sec^{-1}. Each tic mark on the frame enclosing the pattern indicates the location of a horizontal grid point. The obstacle is centered at the long tic marks. The contour representing the obstacle shape is shown as the heavy circle at the origin. The contour shown is one for which the obstacle height is 0.1 the maximum height. The thin lines represent the theoretical wedge angle of the first mode. (Sharman and Wurtele, 1983)

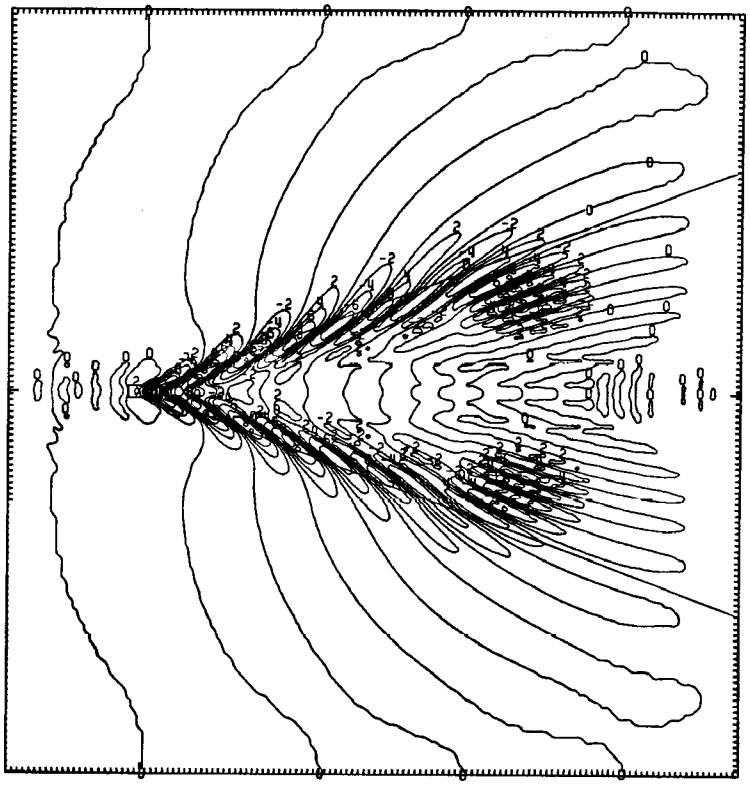

Figure 3. Computer simulation of transient deep water surface ship wave pattern. Contours are surface elevation (cm). Each tic mark on the frame enclosing the pattern indicates the location of a horizontal grid point. Long tic marks indicate the center of the forcing. Lines indicating the theoretical wedge angle of 19.5° are also shown. (Sharman and Wurtele, 1983)

We may pause at this point to look ahead for a moment to inquire as to the sources of malignancy in lee waves, and we shall find that there are three:

(i) Amplification with height owing to the decrease of mean density;
(ii) Forcing of large magnitude, such as by flow over a high mountain;
(iii) Constraint of vertical propagation by a singular level in the atmosphere, such as a reversal of wind direction, so that energy accumulates under this level.

We shall see that the malignancy introduced by each of these causes is characteristic and different from the others.

2. THE DYNAMIC EQUATIONS

We now turn to the analysis of the dynamics of the flows that are the subject of this article, and in the following we shall limit ourselves to two-dimensional atmospheric flow over obstacles infinite and uniform in one direction, taken as the y-direction. The most satisfactory basic treatment is still that of Eliassen and Kleinschmidt (1957). A stratified compressible fluid has four linear modes, two acoustic and two gravity, which are so far apart in their frequencies that it is often convenient to treat them separately. This can be achieved without sacrificing the *static* effect of compressibility, that is the existence of density stratification. The governing equations are then as follows:

$$\frac{\partial}{\partial t}\vec{v} + \vec{v} \cdot \nabla \vec{v} = -\rho^{-1} \nabla p + \vec{g} \tag{1a}$$

$$\frac{\partial}{\partial t}\rho + \nabla \cdot (\bar{\rho}\vec{v}) = 0 \tag{1b}$$

$$\frac{\partial}{\partial t}\theta + \vec{v} \cdot \nabla \theta = 0 \tag{1c}$$

$$\theta = T_0 \frac{\rho_0}{\rho} \left(\frac{p}{p_0} \right)^{\frac{1}{\gamma}} \tag{1d}$$

where γ is the ratio of specific heats, $\gamma = C_p/C_v$. Here the variable that may be unfamiliar is the potential temperature theta, constant in adiabatic processes and equal to the temperature at some arbitrary reference pressure level, usually taken as 1000 millibars. This formulation is called the **anelastic** system (Ogura and Phillips, 1962). It has a serious problem from the point of view of this article in that the prerequisite for an energy integral is that the initial potential temperature distribution is constant. Some progress in relaxing this severe constraint has been made by Lipps and Hemler (1982) and Durran (1989).

A much simpler yet similar system is based on what is known as the **Boussinesq approximation**. This arises from the observation that the role of the density variation in buoyancy, that is, where it is multiplied by gravity, is much more important than as a factor of the acceleration terms. The resulting system takes the form

$$\frac{\partial}{\partial t}\vec{v} + \vec{v} \cdot \nabla \vec{v} = -\nabla \pi + \vec{g}\sigma \tag{2a}$$

$$\frac{\partial}{\partial t}\sigma + \vec{v} \cdot \nabla \sigma = 0 \tag{2b}$$

$$\nabla \cdot \vec{v} = 0 \tag{2c}$$

$$\pi = \frac{p}{\rho_0} \quad , \quad \sigma = \frac{\rho}{\rho_0} \qquad \rho_0 = \textit{constant} \tag{2d}$$

This is a very useful model for fluids in which the total mean percentile density variation is not great. The dynamic consequence of the Boussinesq approximation is easily seen from the non-Boussinesq steady state equations:

$$\rho \vec{v} \cdot \nabla \vec{v} = -\nabla p + \vec{g}\rho$$

$$\nabla \cdot \rho \vec{v} = 0$$

If we now define a new velocity

$$\vec{u} = \sqrt{\left(\frac{\rho}{\rho_0} \right)} \ \vec{v} \tag{3}$$

we have transformed equations in the new velocity u which are identical with the steady-state Boussinesq set (2). Thus if a solution of the Boussinesq equations remains finite as it propagates upward in the atmosphere, a solution without this assumption would grow without limit as z approaches infinity. This effect has been understood for many decades (Lamb, 1932).

Whichever model is used, if the problem is flow over an obstacle, there is a nonlinear boundary condition to be satisfied on $z = h(x)$, where $h(x)$ describes the obstacle in this inviscid model, a purely kinematic slip condition:

$$w(x, h(x)) = udh/dx \tag{4}$$

The implicit character of this condition, except in certain special, idealized situations to be noted later, makes an analytic solution very difficult, and for analytic work this condition is usually linearized in the obvious way

$$w(x, 0) = Udh/dx \tag{5}$$

where U is the mean wind against the obstacle.

3. BENIGN WAVES FOR ZERO MEAN SHEAR

Keeping in mind this very important amplification with height, we will restrict ourselves for the moment to the Boussinesq set (2). And having discarded much interesting compressible dynamics and three-dimensional influence, we may now further assume small sinusoidal perturbations of the form with vector wavenumber $k = (k_1, k_2)$ of the form

$$\exp[i(k_1 x + k_2 z - nt)]$$

When the atmospheric parameters are constant, the dispersion takes a somewhat unusual form, the relative (Doppler-shifted) frequency is

$$n - Uk_1 = Nk_1(k_1^2 + k_2^2)^{-\frac{1}{2}}$$

where N is the buoyancy frequency, defined as

$$N^2 = -\frac{g}{\rho_0}(d\bar{\rho}/dz) \tag{6}$$

Typically the associated buoyancy period in the atmosphere is about 10 min. The corresponding vertical group velocity is

$$G_2 = -Nk_1k_2(k_1^2 + k_2^2)^{-\frac{3}{2}}$$

Thus vertical phase and group velocities are opposite in sign. In atmospheric flow over obstacles, the vertical group velocity must be positive, in order to transport energy upward away from the obstacle. In the steady state, when $n = 0$, we have

$$k_2 = (N^2/U^2 - k_1^2)^{1/2}$$

so that only waves for which k_1 is less than N/U that propagate upward. If U is increasing with height, as is typical in the westerlies, the wave will propagate upward until the altitude is reached at which $k_2 = 0$, then die out exponentially. This case will be discussed in the next section.

For steady-state perturbations, the linearized equations take the form

$$U u_x + U' w = -\pi_x \tag{7a}$$

$$U w_x = -\pi_z - g\sigma \tag{7b}$$

$$U \sigma_x = \left(\frac{N^2}{g} \right) w \tag{7c}$$

$$u_x + w_x = 0 \tag{7d}$$

where $U' = dU/dz$. From these equations, we may infer two important relations (Eliassen and Palm, 1961):

$$\frac{\partial}{\partial z}(\overline{\pi w}) = -U' \overline{uw}$$

$$\overline{\pi w} = -U \overline{uw}$$

The first of these states that averaged over a wavelength, the pressure flux, or rate of working is proportional by the mean velocity to the momentum flux. From the second relation, as is physically evident, a positive rate of working must imply a negative momentum flux, that is, a downward transport of horizontal momentum. From the two equations, we conclude that

$$\frac{\partial}{\partial z}(\overline{uw}) = 0 \tag{8}$$

the momentum flux is independent of height. (Obviously, only the inviscid assumption makes possible a constant momentum flux.) This is a very important result for meteorology, since it is easy to show that

$$\frac{\partial}{\partial t}\bar{u} = -\frac{\partial}{\partial z}(\overline{uw})$$

that is, the mean flow is altered directly by the momentum flux divergence. The benign wave that has achieved a steady state therefore does not interact with the mean flow, although interaction has taken place during the transient development. The momentum flux divergence introduced into the atmosphere by gravity waves is large enough that it must be taken into account by weather prediction models. Without it, over a few days, the simulated jet stream will grow to unrealistic speeds.

Consider a single wave component of wavenumber k with amplitude

$$w(x, z) = \hat{w}(z)\exp(ikx)$$

and similarly for other variables. If these are eliminated, in eqs. (7), in favor of the vertical velocity w, there results

$$\hat{w}'' + \left(\frac{N^2}{U^2} - \frac{U''}{U} - k^2 \right) \hat{w} = 0 \tag{9}$$

an equation first derived by Scorer (1949).

The theory of atmospheric lee waves began just 50 years ago with G. Lyra (1943). Assuming in (9) a constant N and a constant U, Lyra composed by means of a Green's function solution the gravity waves represented to fit a doublet lower boundary condition. Lyra's original graph of his solution is presented in Figure 4. The analytic expression for the result is rather complicated, consisting of an infinite series of Bessel functions; but its asymptotic far-field expansion for the *downwind* side of the doublet is very simple:

$$w \sim -Uh^* \frac{z^*}{r^*} \sin\left(r^* - 3\frac{\pi}{4}\right)$$

Here r is the radial distance from the origin, and the distances r^* and z^* are dimensionless, having been scaled by N/U. It is seen that the phase lines Nr/U = constant are semicircles. The upstream slope of these phase lines satisfies the condition of downward momentum flux, and the fall-off with distance r represents the spreading of the wave energy in two dimensions.

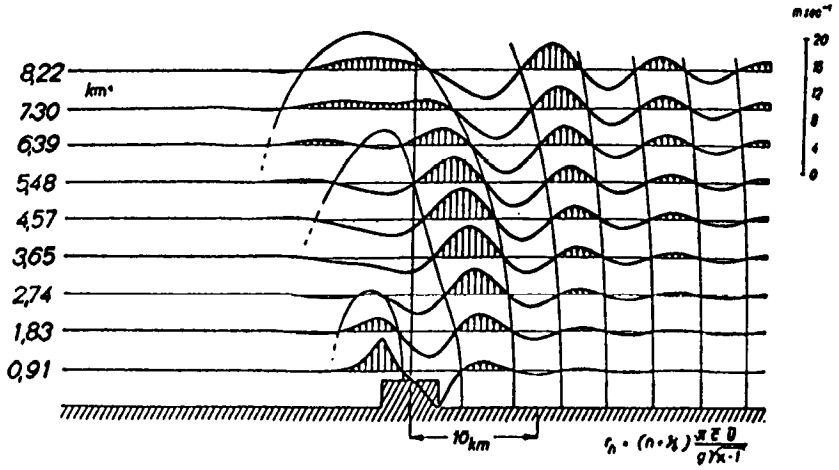

Figure 4. Vertical velocity field for flow over a doublet. Initial mean wind is constant and stability is also constant. (Lyra, 1943)

4. GROWTH OF A MALIGNANCY

This granddaddy of all atmospheric lee waves—that is, those resulting from the atmosphic structures first treated by Lyra (1943) and Queney (1948)—has never, to my knowledge, been documented by observations from nature, whether because the wind speed in nature refuses to remain constant with height, or because the moisture at higher levels is insufficient to visualize the characteristic upwind tilting pattern. In any case, in theory or in nature, this would seem to be a truly benign wave, with amplitude falling off both downstream and with elevation. However, we must remember that this solution satisfies the Boussinesq equations, and we still have the exponential amplification effect contained in equation (3). A rough calculation, given a (constant) scale height for the mean density of, say, 8 km, shows that amplification by a factor of 50 to 100 will take place from about 60 to 90 km elevation. This should be sufficient to produce a malignancy in even the smallest tropospheric perturbation. Some recent simulations by Bacmeister and Schoeberl (1989), Figure 5, show that an upward-propagating small amplitude wave does in fact break down, and that the chaotic region then propagates downward. It should be pointed out, however, that the precise dynamic mechanism by which this occurs, and the character of the chaotic flow and its transition into turbulence, have not been thoroughly investigated and are not understood. This point will be emphasized later in connection with waves in the middle atmosphere.

The Lyra lee wave is also subject to the second type of malignancy, due to large forcing, a topic that has received a great deal of attention in the literature. It was shown by Long (1955) that for this special case, U and N constant, the nonlinear terms vanish identically, and therefore a solution of the linear equation is valid

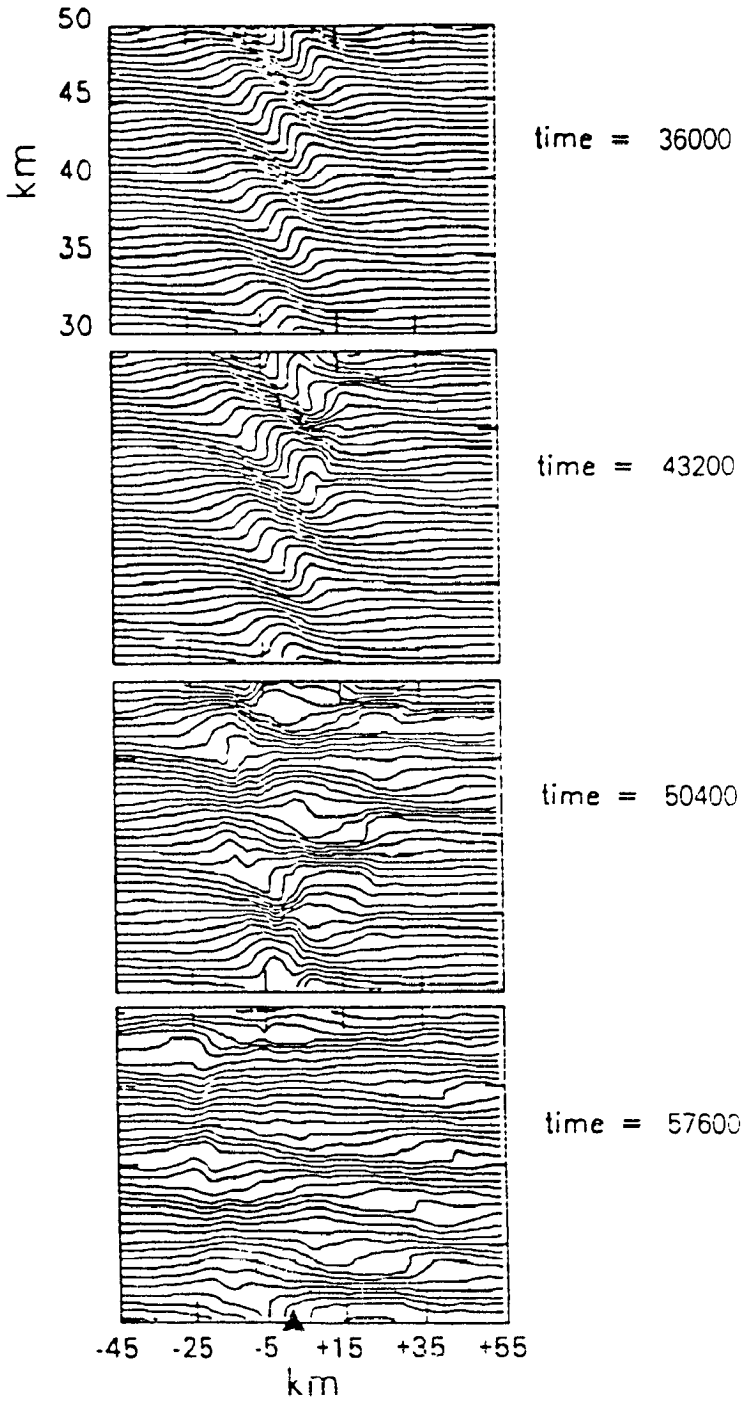

Figure 5. Potential temperature as a function of *x* and *z*. Time increases from top to bottom. Contour interval is 3 K. Position of ridge crest is indicated by black triangle in bottom frame. (From Bacmeister and Schoeberl, 1989)

for any amplitude. This provided a field day, or rather a field decade, for applied mathematicians. The solutions are not trivial, since it is still required to satisfy the nonlinear kinematic boundary condition. Similarity theory suggests, and dynamic analysis confirms (see equation (10)), that the condition for potential malignancy in this model is

$$h^* = Nh/U = O(1)$$

The precise critical value of h^*—which is obviously an inverse Froude number—depends on the shape of the obstacle. When this critical value of h^* is attained or exceeded, some streamlines will have vertical or negative slope, that is, where the horizontal component of the (total) flow velocity is zero or negative. In the steady state solution, density contours coincide with streamlines, so that the vertical density gradient is zero or positive. In nature, overturning must ensue, and the model as presented above ceases to be valid. The most complete analytical treatment of this situation is that of Huppert and Miles (1969), one solution from which is diagrammed in Figure 6.

Figure 7 is an often-reproduced photograph of this phenomenon in the lee of the Sierra Nevada. The dust rising off the floor of the Owens Valley visualizes the reversed flow and what is called the **rotor cloud**. This region is, of course, extremely turbulent. The strong downslope winds, equally turbulent, can be damaging to structures at the base of the mountain. An example of a site especially subject to downslope windstorms is Boulder, Colorado, where peak gusts in excess of 100 mph have been recorded. This phenomenon has been well observed and documented in a number of articles, notably Lilly (1978). (A simulation of this situation is presented later in Section 6.) It cannot be said, despite the energy devoted to the study of this spectacular phenomenon, that it is completely understood. It occurs only a few times per year, yet the conditions for its occurrence would seem to be much more common. What triggers the violent conditions has not been satisfactorily identified, although Clark and Peltier (1984) have made a valiant attempt that will be referred to later.

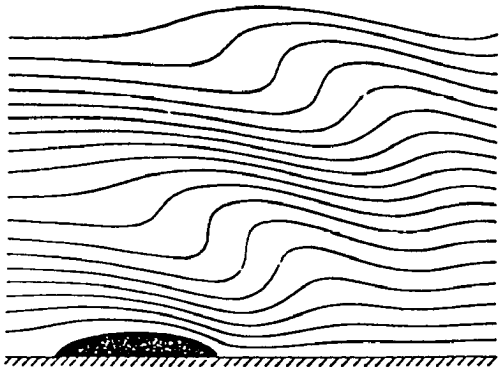

Figure 6. Streamlines for stratified flow over a half-ellipse with $Nh/U = 0.9$: analytic solution of Huppert and Miles, 1969.

Figure 7. Strong wave in the lee of the Sierra Nevada, looking southward along Owens Valley. The intense downslope winds arc picking up dust from the valley floor and carrying it up into the rotor cloud, indicating a reverse circulation in the valley, similar to a hydraulic jump on an interface. Photo by Bob Simons.

5. BENIGN (TRAPPED) WAVES IN SHEARING FLOW

We shall now turn to a second type of benign wave pattern. Suppose we relax the restriction that the mean flow is constant, and allow it to increase with height. In order to simplify the model, let the shear $U' > 0$ be constant. The vertical structure equation is then

$$\hat{w}'' + \left(\frac{Ri}{z^2} - k^2 \right) \hat{w} = 0 \tag{10}$$

Here a new parameter has been introduced, the Richardson number

$$Ri = N^2/(U')^2$$

or the ratio of the buoyancy to the shear. Mathematically speaking, this equation has a turning point at

$$z = \sqrt{Ri}/k$$

and a singularity at $z = 0$, where the mean flow vanishes.

The behavior of the solution will obviously be very different at these two points. First consider the case for which $U > O$ throughout the domain of the model, and for which $Ri >> 1/4$, so that Kelvin-Helmholtz instability is not present. It may be noted that the term in k^2 represents the vertical accelerations; neglecting this term corresponds to making the assumption that the disturbance is hydrostatic: no turning point, vertical oscillations to infinity, no horizontal waves.

The solution of (10) regular at all values of z including infinity is

$$\hat{w} = \sqrt{kz} K_{iq}(kz) \quad \text{where} \quad q = \sqrt{(R_i - 1/4)}$$

Here K is a Bessel function of imaginary order and imaginary argument, real for real argument. It is oscillatory for argument less than order and exponentially decreasing for argument greater than order. It is described and graphed in Wurtele et al. (1988), where references to the earlier literature are given. For realistic values of the Richardson number, this function has multiple zeros, from which it follows that for a given level of forcing, say $z = z_1$, there will be one or more wave numbers, say $k = k_1$, for which resonance waves will be forced. They will be of the form

$$w \sim \sqrt{k_1 z} K_{iq}(k_1 z) \ \sin\ (\mathrm{k}_1 x) \tag{11}$$

that is, an infinite train of vertically oriented cells. These are called **trapped waves**, since the energy does not propagate vertically, but only downstream. An illustration for an instance in which only a single wave is excited is presented in Figure 8. Satellite imagery has taught us that the trapped lee wave is a fairly common phenomenon in nature; for example, Figure 9 shows an instance in which the wave train extends more than a thousand miles.

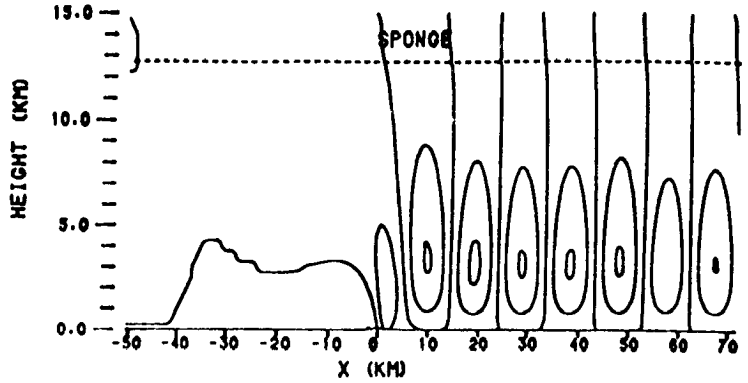

Figure 8. Trapped wave forced by a witch of Agnesi profile cells of vertical velocity (contours 0.2 m/sec) at time 14,000 sec (Ri = 8). (From Wurtele et al., 1987)

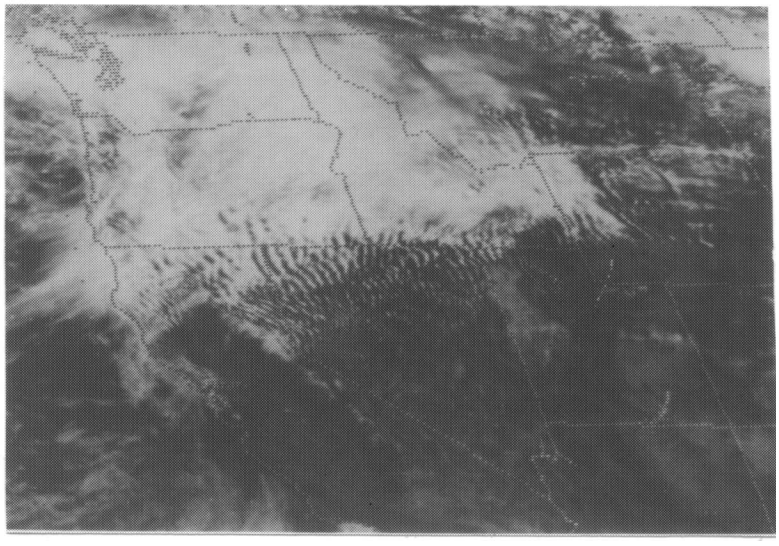

Figure 9. Satellite imagery showing lee waves originating from coastal and southern Sierra Nevada range of California.

The trapped wave is obviously not subject to malignancy of the first kind—that is, due to decrease of mean density—since its vertical propagation is by definition limited. It is, of course, subject to breakdown in nonlinear forcing, but there is a slight ambiguity here: Nh/U is no longer the only dimensionless group to be considered; $U'h/U$ also qualifies. The question of the roles of these two parameters has never been properly posed and answered, perhaps because no one has ever demonstrated the development of a significant difference in the onset of nonlinearity by the addition of shear to a model.

We now turn to a very different dynamic situation. Let the motion be governed by (10) as before, but let the singular point $z = 0$ be within the field of flow, that is, let the mean flow reverse its direction at some level above the obstacle. Since we are seeking disturbances stationary with respect to the obstacle, the level $z = 0$ is that at which the wave speed is equal to the current speed (in this case, zero), known in hydrodynamics as a **critical level**. The appropriate formal Bessel function solution to equation (10) is

$$\hat{w} = \sqrt{kz} I_{iq}(kz)$$

but since this is not physically meaningful at $z = 0$, we must consider the transient state. It was noted by Bretherton (1966) and Booker and Bretherton (1967) that the vertical group velocity for an upward propagating wave in this medium, assumed "slowly varying," is proportional to $(n - kU)^2$, and the vertical wave number is proportional to $(n - kU)^{-1}$, so that as the wave approaches the critical level, $U = 0$, it slows toward zero group speed and its vertical wave length decreases toward zero. The wave can never become steady, nor can it reach or penetrate the critical level, so that the wave energy accumulates beneath it. Some sort of breakdown is inevitable, and the form it takes must be determined either by nonlinear analysis or by numerical simulation. Brown and Stewartson (1982) and Grimshaw (1988) attempt this very difficult analysis, but we find that simulation provides more information. An example is presented in Figure 10. In Figure 10(a), at time step 300, the fields are still linear, approaching the (singular) solution (11). The details of the breakdown are examined in Landau and Wurtele (1992), but from Figure 10(b) it is clear that higher harmonics have been generated near the critical level and are propagating downward. The final (and predictable) outcome in this inviscid model is the equipartition of energy among all wave components that can be resolved by the numerical scheme. This is a highly idealized model of forcing by a single wave component; when the flow is forced over a limited two-dimensional obstacle, the result is that pictured in Figure 11. The upwardly propagating disturbance sees the critical level as a barrier, and there is no dynamic mechanism for downstream propagation, so that the breakdown occurs, and no matter how fine the computation grid, the dynamic mechanism will generate motions too small to be resolved by it. This is a situation demanding a rational, consistent parameterization of turbulence.

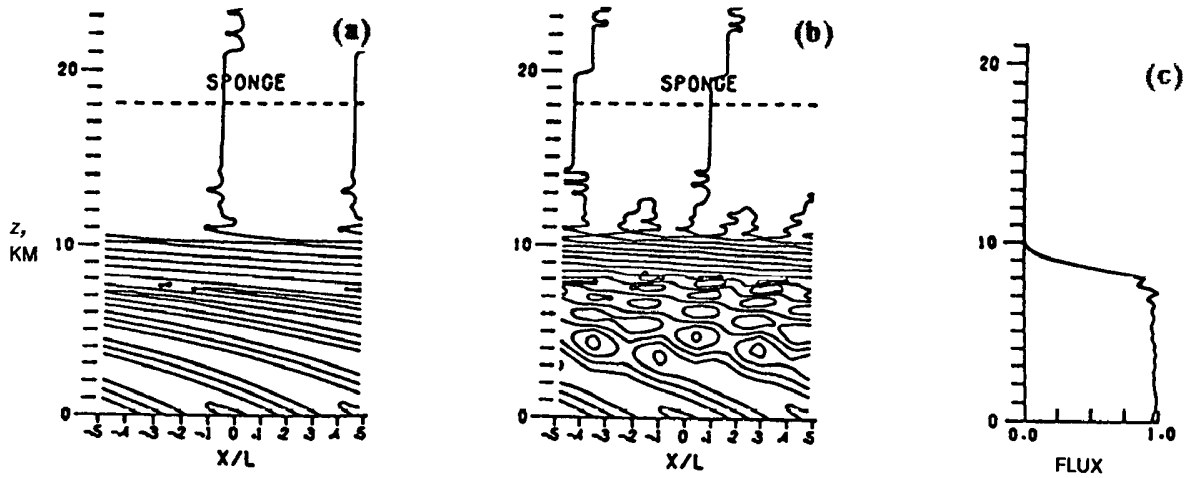

Figure 10. Simulation of gravity wave for $Ri = 100$, forced toward a critical level at $z = 10$ km. (a) Linear stage (400 time steps, 3.3 hr). (b) Nonlinear scattered stage (600 time steps, 5 hr). (c) Nondimensional momentum flux profile at 600 time steps. $\Delta t = 30$ sec, $U_0 = 10$ m/sec, $U' = 10^{-3}$ sec^{-1}. (Wurtele et al., 1992)

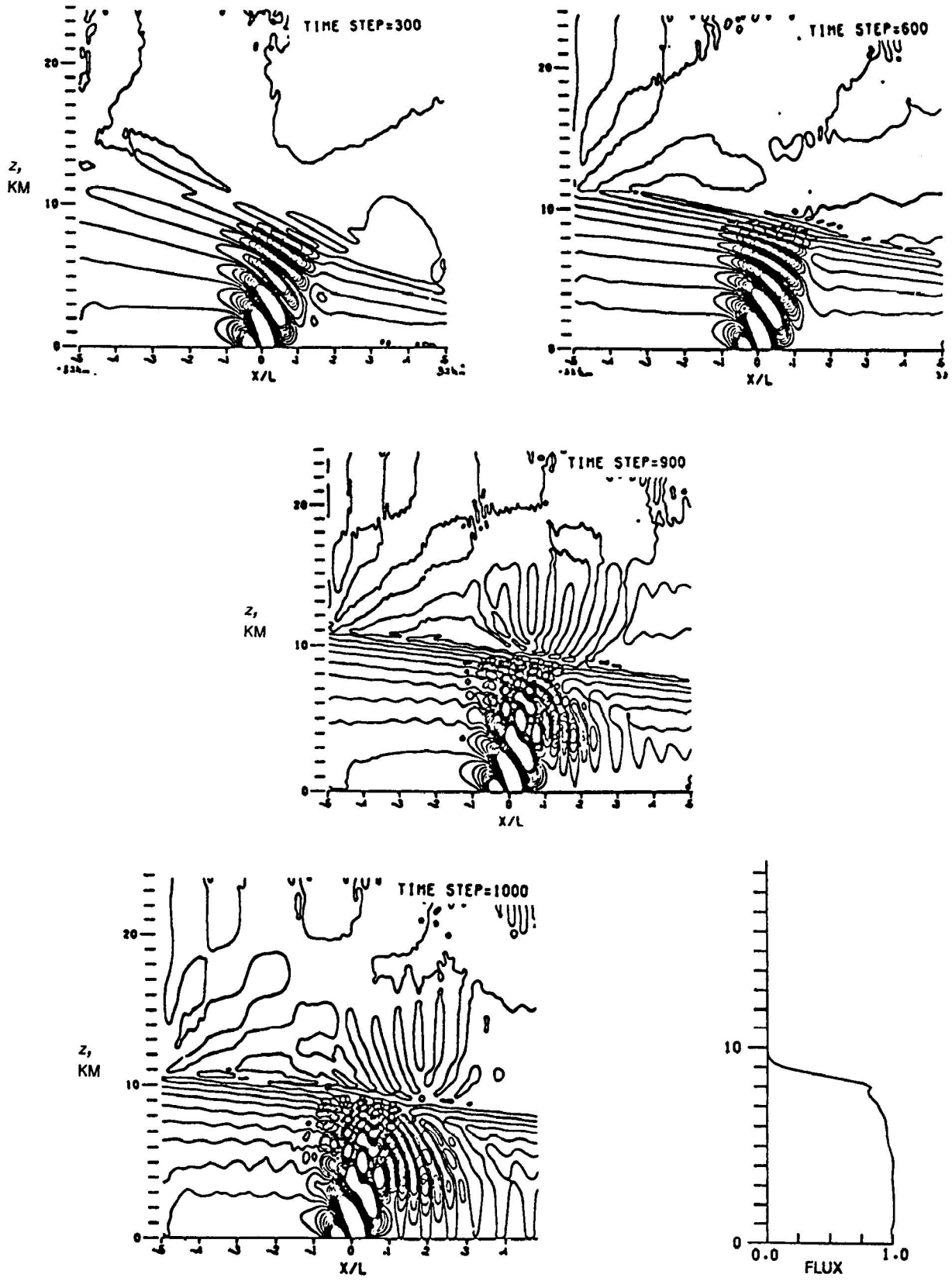

Figure 11. Simulation for *Ri* = 100 of lee disturbances resulting from backscatter of gravity waves from a critical level (*z* = 10 km) at successive time steps and associated nondimensional momentum flux profile at 1000 time steps, Δ*t* = 30 sec. (Wurtele et al., 1992)

A dramatic example of the critical level dynamics in nature was the Arvin-Bakersfield dust storm of December 20, 1977. An easterly wind blew over the Tehachapi Range, reversing at about 4.5-km elevation to westerly. The result in the San Joaquin Valley was a violent windstorm, raising a dense dust cloud to an elevation of 1.5 km, not only causing damage to property, but acting as a serious public health hazard. However, in nature, the most frequently encountered critical level occurs in a more complex situation, in the stratosphere, above a troposphere in which the wind has increased with height. Well-documented cases of this phenomenon exist for the Sierra Nevada in California and for the Front Range of the Rockies in Colorado. Clark and Peltier (1984) suggest that even though the stratospheric wind direction reversal is at an elevation of greater than 9 km, the strong downslope winds and associated clear air turbulence in the troposphere do not occur without it. Our own studies tend to confirm this observation, although the dynamics of this relationship is not clear.

At this point we should mention the efforts that have gone into field experiments to characterize the benign and especially the malignant lee waves. In these, extensive surface networks and special sounding schedules have been supported by radar, aircraft, and sailplane observations, involving the collaboration of many organizations and private individuals. The strength of the waves is evidenced by the altitudes achieved by the (unpowered) sailplanes, 12 to 15 km, with a ceiling here only because oxygen equipment is not designed to operate at such low ambient pressures.

Among these may be cited the first such major, cooperative experiment, the Sierra Wave Project (Holmboe and Klieforth, 1956), followed by a number of investigations of the Colorado waves (Lilly, 1978). An entire international experiment of the World Meteorological Organization, ALPEX, was devoted to the exploration of Alpine lee waves. Currently, a European group is putting together a study of the Alpine Foehn. It has become important that such field experiments concern themselves with the connection, if any, between lower and middle atmospheric disturbances, as will become clear in Section 7.

6. THE SIMULATION OF LEE WAVES

Even in linear models realistic atmospheric conditions produce intractable problems, and for most of these conditions, nonlinearities cannot be ignored. Although there have been attempts at laboratory experiments, numerical simulation has become the methodology of choice in attempting to represent flow over earth terrain. Since the first such simulation (Foldvik and Wurtele, 1967), some rather elaborate models and techniques have been developed, and a brief account of certain of the features of these may be of interest.

As mentioned above in Section 2, a major problem is the failure of the anelastic set (1) to conserve energy under all conditions. Two numerical procedures have been advanced to mitigate this defect, one by Lipps and Hemler (1982) and one by Durran (1989). The former assume mean potential temperature to be "slowly varying" with height, and to the extent that this is true, energy is conserved. However, in the stratosphere the variation is normally rapid, and the model requires testing under this condition. Durran proposes a revised version in which

$$\nabla \cdot (\bar{\rho}\bar{\theta}\vec{v}) = 0$$

is the continuity equation for purely adiabatic flow, with no restrictions on the distribution of the mean quantities. This system conserves a form of energy closely related to the "true" energy. However, it becomes necessary to solve a very complicated and messy elliptic equation.

The problem of satisfying exactly the lower boundary condition is one that has been approached in two ways. One is to retain a Cartesian grid, and to represent the obstacle by a series of blocks with sides the size of the grid. There is a question of whether a series of little impulses can properly represent the effect of a smooth slope, and for this reason, researchers turned to methods by which the terrain itself could become a coordinate surface. The usual way of achieving this is to define a new vertical coordinate

$$z^* = [z - h(x)]/[H - h(x)] \tag{12}$$

that is zero along the bottom boundary and unity along the top ($z = H$). This works well in a number of models, but is subject to a penalty in computation for the following reason. Unless the model is fully compressible, including the acoustic modes, there will be an elliptic equation for the pressure or for the stream function to solve at each time step. Normally this is a simple Poisson equation, easily amenable to block cyclic reduction techniques. However, the transformation (12) determines a coordinate system that is not orthogonal, with the result that the elliptic equation for the pressure becomes horrendously messy, with cross-differentiation terms. With this difficulty in view, Sharman et al. (1988) developed a numerical grid generation scheme of the sort that is very familiar to aeronautical engineers, that preserves orthogonality and the form of the Poisson equation. Two examples of the working of this scheme are presented in Figures 12 and 13. Figure 12 reproduces the flow over an ellipse, chosen for the challenge of the right-angle kink in the streamline, and is to be compared with the analytical result in Figure 6. Figure 13 shows the flow over a numerically assigned profile of the Sierra Nevada, with typical winter storm initial conditions, and is to be compared with Figure 7.

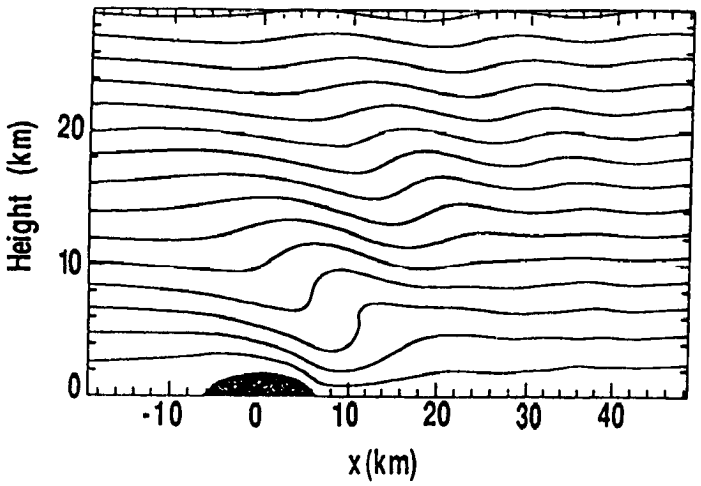

Figure 12. Streamlines for stratified flow over a half-ellipse with *Nh/U*=0.9: simulation using terrain-following grid generation code (from Sharman et al., 1988).

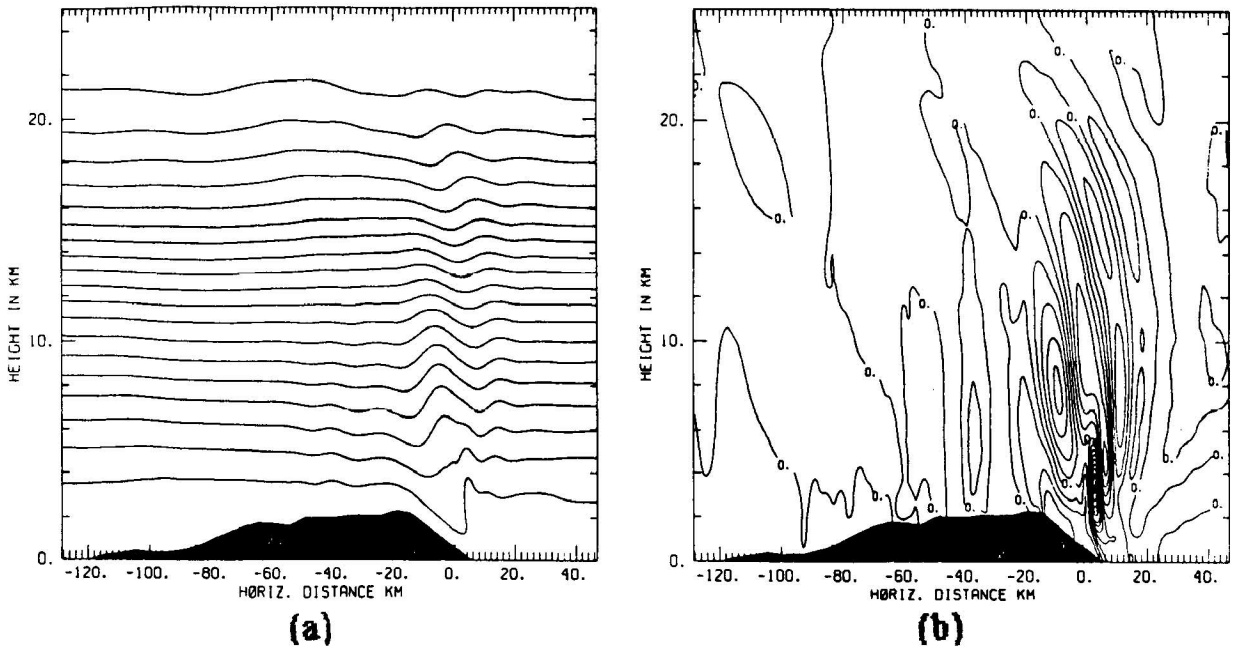

Figure 13. (a) Streamlines for flow over digitized profile of the Sierra Nevada, with typical winter storm initial conditions. (b) Contours of vertical velocity (1 m/sec^{-1}) corresponding to (a). (Sharman et al., 1988)

As examples of simulations by other groups with other codes, we may cite Peltier and Clark (1983), Klemp and Lilly (1978), and Durran and Klemp (1983). A recent project sponsored by NASA Dryden Flight Research Facility and managed by L. J. Ehernberger has specified six sets of terrain profiles and associated sets of observed initial conditions for "blind" simulations by five different codes, in order to assess the comparative simulation results—the first ever test of this kind. The various runs are now under evaluation.

7. MIDDLE ATMOSPHERE DISTURBANCES

For many years the primary emphasis of researchers on lee waves was on the structure of the disturbance in the troposphere and lower stratosphere—not coincidentally, the region from which observations from sailplanes and powered planes were available, and in which visualization was possible by means of cloud formations. A pioneering effort to direct attention to higher atmospheric levels was that of Hines (1960), followed by many articles by ionospheric workers. For example, Yeh and Liu (1972) treat problems of ionospheric disturbances of presumably gravity wave origin. The chief means of detection was by ionosonde. Since the ionosphere normally begins above 100 km elevation, this left the region between about 20 or 30 km to 100 km unexplored. This region has become known as the **middle atmosphere**, and its exploration at that point in time awaited the development of adequate observation and measurement technology.

Early (and not so early) radar engineers were annoyed when weather in the form of precipitation elements – known to them as "weather noise"– interfered with the return signals from aircraft, and were later outraged when even clear air contributed to this noise. One person's noise being another person's signal, meteorologists were quick to adopt radar as one of their most valuable probes, ground based, airborne, and

spaceborne. The extent of use of this versatile tool in atmospheric research is impressively recorded in the recent collection by D. Atlas (1990), with surveys of UHF/VHF instrumentation, monostatic and Doppler, by Roettger and Larsen (1990) and of their use in clear-air probing by Hardy and Gage (1990) and Gage (1990). The development of middle-atmosphere radar came to fruition in the late 1970s and 1980s, and for the past decade, the bulk of articles published on gravity waves—one can scarcely call them lee waves without some evidence that they are in the lee of some specified source—has been concerned with middle atmospheric disturbances. Typically a radar can provide only a time sequence of vertical profiles of scatterers, or a Doppler radar with a profile of velocities. Thus information as to the vertical wave length is much more abundant than information about the horizontal wave length. The radar yields many such profiles, so that statistics are available in the form of vertical spectra, and there is considerable evidence that these energy spectra follow the power law

$$E(m) = A\, m^{*-1}\, [1 + (m/m^*)^3]^{-1} \tag{13}$$

where m is the vertical wavenumber, and m^* is a scaling parameter, different for troposphere, stratosphere and mesosphere. (Tentatively, one may take m^* as 1, 0.2, and 0.05 cy/km, respectively.) Figure 14 provides an example of a data set conforming to this spectral distribution. From the form of (13), it is evident that the "energy content" spectrum, $mE(m)$, has a maximum for m equal to about 0.8 m^*. For the middle atmosphere, this locates the maximum power in the spectral range of gravity waves; and a simple dimensional argument suggested that m^{-3} is the form an energy spectrum would take in a regime of wave-breaking, called **saturation**. This observational result resonated with theoretical arguments (e.g., Lindzen, 1981) that breaking in the middle atmosphere was to be expected, owing to the first mechanism, amplification due to decreasing density with height, as discussed in the introduction.

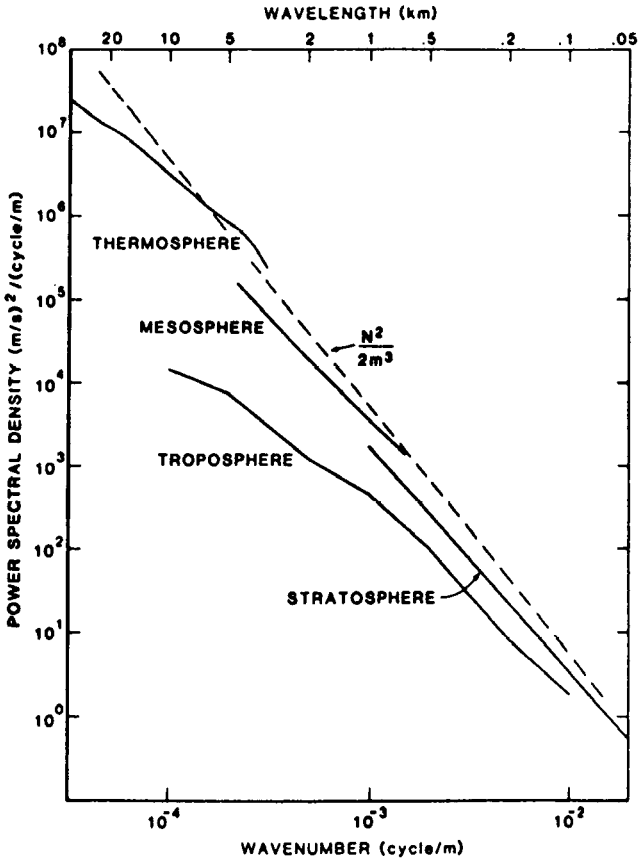

Figure 14. Spectra of horizontal velocity versus vertical wave number as a function of altitude. (Smith et al., 1989)

However, this is a large leap to be achieved by what is essentially a wave of the arm, and there remains considerable disagreement. The literature in this area is now voluminous. Review articles by Fritts (1984) and Dunkerton (1989) provide some orientation; most issues of the *Journal of Geophysical Research* now contain articles on this or related problems.

There is some information available on the horizontal scale of these middle atmosphere disturbances. The space shuttle reenters the atmosphere at a small inclination to the horizontal, and its accelerations are recorded. From these, variations in drag, and hence in air density, can be inferred. Indirect as this evidence is, it presents a reasonable and consistent picture. Figure 15 shows a horizontal spectrum derived from seven reentries by Fritts et al. (1989). These results suggest that two orders of magnitude of wavelength, from 10 to 1000 km, are present in the middle atmosphere disturbance spectrum. Supporting data are provided by Fetzer (1990) in an analysis of limb-scanning IR measurements. Fetzer calculates no spectra, and he can report only temperature variations; but it is clear that horizontal scales up to 1000 km, and vertical scales of the order of 10 km, are present. And the excursions are very large: up to 20° C.

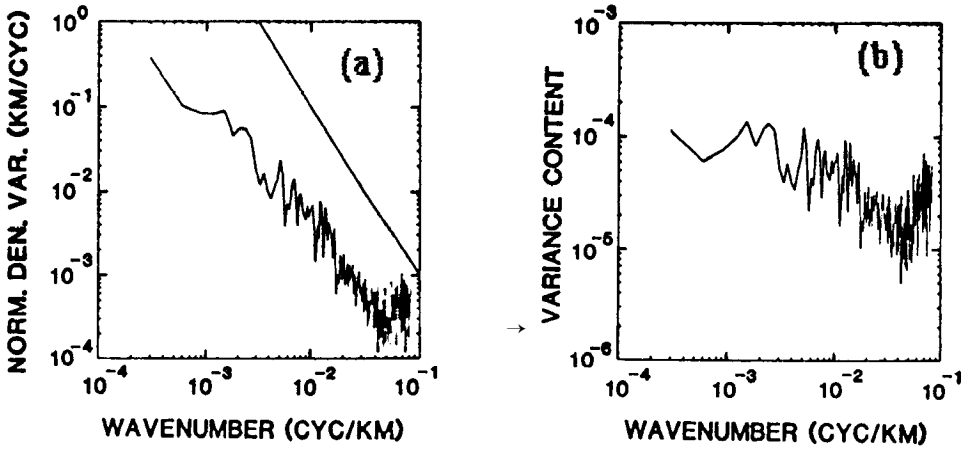

Figure 15. Mean horizontal wavenumber spectrum for the seven reentries in (a) standard and (b) variance content form. A slope of –2 is shown for reference in (a). (Fritts et al., 1989)

As was anticipated theoretically, scales of this magnitude alter the rules of the game. When the time scale, here taken as the length scale divided by the wind speed, is of the order of the pendulum day, the rotation of the earth must be accommodated in the dynamics, and the equations (l) become altered by the addition of a Coriolis acceleration, which meteorologists write as

$$f\vec{k}\times\vec{v}$$

The **Coriolis parameter** f is the rate of rotation of the Earth about the local vertical—about 10^{-4} per second in middle latitudes—and k is the local vertical unit vector. Of course, f will vary with latitude, but the scale of these disturbances is still too small to be affected by this variation. Thus f will be taken as constant, and the perturbations arising out of this model are called **inertia-gravity waves**. It should be remembered that in the middle atmosphere kinematic viscosity and conductivity, both inversely proportional to density, will play a role in the dynamics of scales of motion for which they would be totally negligible at lower altitudes. Thus we are not attempting here to simulate middle-atmosphere disturbances,

but to inquire into the dynamics of vertical propagation to determine the conditions under which gravity and inertia-gravity waves will or will not actually propagate to these levels—assuming for the moment that their source lies at lower levels.

We will not write out the nonlinear equations as modified by the Coriolis term, noting only that the growth in amplitude with decreasing density holds just as it did for gravity waves, and thus the middle atmosphere is as vulnerable to wave-breaking and turbulence with inertia-gravity waves. However, the Boussinesq dynamics are considerably altered (Jones, 1967). Equation (10) is replaced by

$$\left[z^2 - \left(\frac{f}{kU'}\right)^2\right]\hat{w}'' + \left(\frac{2f^2}{k^2U'^2z}\right)\hat{w}' + (Ri - k^2z^2)\hat{w} = 0$$

Here the single singularity at $z = 0$, multiplying only the first order derivative, has become innocuous, but two new singularities at

$$z = \pm\frac{f}{kU'} \tag{14}$$

have been introduced. This equation is amenable to analysis (Grimshaw, 1975; Tanaka and Yamanaka, 1984; Wurtele et al., 1991), the solution being the hypergeometric function, and it is not difficult to show that a monochromatic wave impinging on the lowest singular level from below will exhibit a behavior quite similar to that of Figure 10. However, as with the case of the gravity-wave critical level, simulation shows results that are not anticipated by analysis. There is a major difference from the critical level, in that the level of the singularities (14) depend on the horizontal wavenumber k, so that when the disturbance is forced by a *continuous spectrum*, each component will have its own singular level. We should not expect for inertia-gravity waves, then, the explosive behavior characterizing the critical level for gravity waves, as represented in Figure 10(b). Corresponding to this situation we now have that of Figure 16, in which there is neither wave-trapping, nor nonlinear reflection, but rather an increase in horizontal scale as the disturbance propagates upward. There is no indication of malignancy.

We have yet to consider disturbances originating between the singular levels (14). Linear theory shows, and simulation confirms, that upward propagation is greatly inhibited in this regime. However, if the perturbation has sufficient energy to reach the zone beyond all critical levels, we find a startling behavior. This should be a situation in which the system seeks to find a resonant trapped wave lee wave, as in Figure 8, but the linear solution provides none. What the simulation shows (Figure 17) is that, despite the fact that the forcing is steady, the response is a periodic “lee” wave, where the quotation marks are required because during phases of the period, different sides of the obstacle are acting as “lee.” Since once it has escaped beyond the singular level, the wave may propagate freely upward, this result may be of some importance in middle atmospheric dynamics.

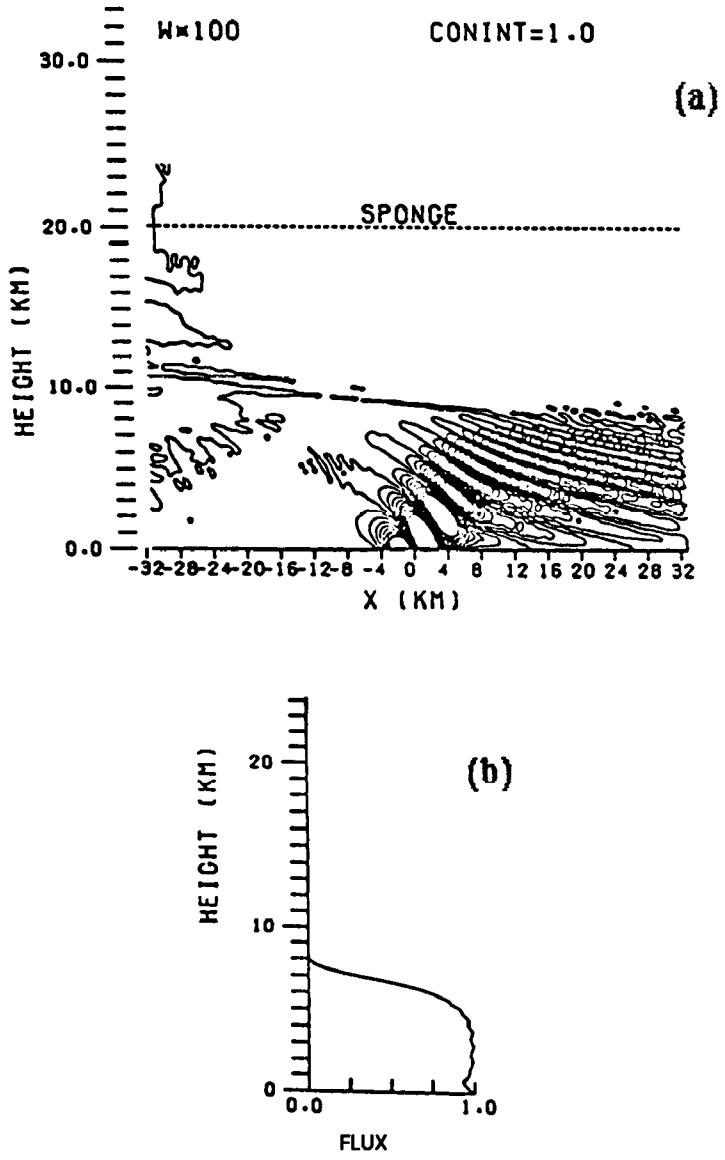

Figure 16. Simulation of lee wave resulting from backscatter of inertia-gravity waves from their associated singular levels for R_i = 100. (a) Vertical velocity field at time step 1000 (Δt = 20 sec). (b) Nondimensional momentum flux profile corresponding to (a). (Wurtele et al., 1992)

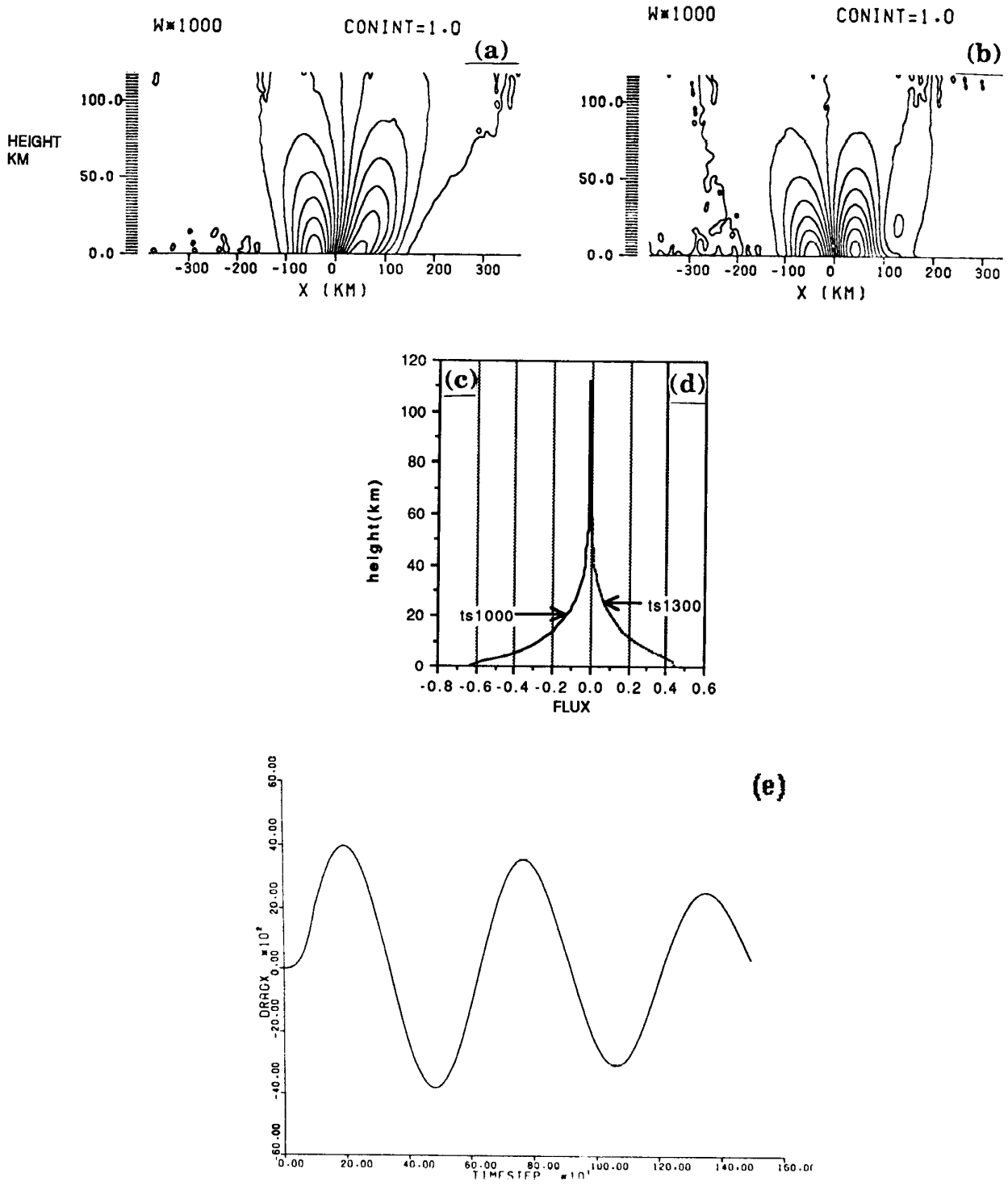

Figure 17. Gravity-inertia wave (*Ri* = 100) forced by an obstacle of Gaussian profile. (a,b) Contours of vertical velocity (m/sec) at time steps 1000 and 1300 respectively. (c,d) Height profiles of momentum flux at times corresponding to 6(a,b). (e) Time-profile of drag to 1600 time steps. The decrease of amplitudes is part of a longer-period fluctuation. (Wurtele et al., 1992)

8. LOOKING FORWARD

Future research in gravity and inertia-gravity waves will probably be dominated by the study of disturbances in the middle atmosphere, for several reasons. First, this is the region in which there will be the greatest incidence of new and exciting observations. Not only are the number of radars and lidars increasing that are capable of sounding to high altitudes, but high-performance aircraft are now penetrating into the middle stratosphere, and, in the case of the shuttle, upper stratosphere, returning data, and presenting practical motivation for an understanding of these atmospheric layers. In fact, such aircraft, properly instrumented, will be used as probes to study the region. If there is, in fact, a National Aerospace Plane in our future, it will have to traverse the middle atmosphere. And planes traveling at Mach numbers five to ten, or even more, times those of commercial aircraft will sense perturbations of scales never before thought of as potentially impacting aircraft.

The analysis of inertia-gravity waves, and even more, their simulation, offer many unsolved and probably unanticipated problems. Observations alone will not tell us the origin of the middle atmosphere disturbances; they must be interpreted in terms of the theoretical models, as realized in nonlinear simulations. Is the source at the surface of the earth; does it lie in fronts and storms; is it due to disequilibria of the jet stream; is it all of these, or in some phenomenon that no one has yet mentioned in this connection?

One of the major problems confronting numerical weather prediction and climate models has been, and will for a time continue to be, the incorporation of the atmosphere above the tropopause. As mentioned above, the momentum flux convergence produced by gravity waves is now an essential parameterization in weather prediction. Similarly, the flux fields, momentum and temperature, of inertia-gravity scale in the middle atmosphere will be important in the circulation of that region. This question is inevitably linked with that of the breakdown of these waves and the formation of and character of the resulting turbulence. Modeling of this problem has begun, e.g., Gavrilov and Yudin (1992), and we will probably soon see some of the huge, computer-intensive turbulence code simulations in this context that we have recently seen for problems associated with boundary layer flow and convection.

So there is plenty of work for a wide range of talents, scientists and engineers, experimenters, and theoreticians. Everyone is welcome to participate.

9. ACKNOWLEDGMENTS

The authors gratefully acknowledge the valuable comments and other assistance of Dr. D. M. Landau and Mr. L. J. Ehernberger. This research was sponsored under Grant NCC2-374 from NASA Dryden Flight Research Facility.

10. REFERENCES

Atlas, D. (ed.), 1990: *Radar in Meteorology*, American Met. Soc. (publisher), 822 pp.

Bacmeister, Julio T. and Schoeberl, Mark R., 1989: “Breakdown of vertically propagating two dimensional gravity waves forced by orography,” *J. Atmos. Sci.*, 46, pp. 2109–2134.

Booker, J.R. and Bretherton, F.P., 1967: “The critical layer for internal gravity waves in shear flow,” *J. Fluid Mech.*, 27, pp. 513–539.

Bretherton F.P., 1966: “The propagation of groups of internal gravity waves in shear flow,” *Quart. J. Roy. Met. Soc*., 92, pp. 466–480.

Brown S.N. and Stewartson K., 1982A,B: “On the nonlinear reflection of a gravity wave at a critical level, Part 2 and 3,” *J. Fluid Mech.*, 115, pp. 217–251.

Clark, T.L. and Peltier, W.R., 1984: “Critical level reflection and the resonant growth of nonlinear mountain waves,” *J. Atmos. Sci.*, 41:21, pp. 3122–3134.

Dunkerton, T.J., 1989: “Theory of internal gravity wave saturation,” *Pure and Appl. Geophys*., 130, pp. 373–397.

Durran, D.R. and Klemp, J.B.: “A compressible model for the simulation of moist mountain waves,” *Mon. Wea. Rev.*, 111, pp. 2341–2361.

Durran, D.R., 1989: “Improving the anelastic approximation,” *J. Atmos. Sci*., 46, pp. 1453–1461.

Eliassen, A. and Palm, E., 1961: “On the transfer of energy in stationary mountain waves,” *Geofys. Publik*. 22:2.

Eliassen, A. and Kleinschmidt, E., 1957: “Dynamic meteorology,” in *Handbuch der Physik XLVIII*, Springer Verlag, Berlin.

Fetzer, Eric Jospeh, 1990: “A global climatology of middle atmosphere inertio-gravity waves,” Doctoral dissertation, Univ. of Colorado.

Foldvik, A. and Wurtele, M.G., 1967: “The computation of transient gravity wave,” *Geophys. J. R. Astron. Soc*., 13, pp. 167–185.

Fritts, D.C., 1984: “Gravity wave saturation in the middle atmosphere: A review of theory and observations,” *Rev. Geophys. Space Phys*., 22, pp. 275–308.

Fritts, David C., Blanchard, Robert C., and Coy, Lawrence, 1989: “Gravity wave structure between 60 and 90 km inferred from space shuttle entry data,” *J. Atmos. Sci*., 46:3, pp. 423–434.

Gage, K.S., 1990: “Radar observations of the free atmosphere: structure and dynamics,” in *Radar in Meteorology*, American Met. Soc. (publisher), D. Atlas (ed.), pp. 534–565.

Gavrilov, Nikolai M. and Iudin, Valerii A., 1992: “Model for coefficients of turbulence and effective Prandtl number produced by breaking gravity waves in the upper atmosphere,” *J. Geophys. Res*., 97:D7, pp. 7619–7624.

Grimshaw, R., 1975: “Internal gravity waves: critical layer absorption in a rotating fluid,” *J. Fluid Mech*., 70, pp. 287–304.

Grimshaw, R., 1988: “Resonant wave interactions in a stratified shear flow,” *J. Fluid Mech*., 190, pp. 357–374.

Hardy, K.R. and Gage, K.S., 1990: “The history of radar studies of the clear atmosphere,” in *Radar in Meteorology*, American Met. Soc. (publisher), D. Atlas (ed.), pp. 235–281.

Hines, C.O., 1960: “Internal atmospheric gravity waves at ionospheric heights,” *Can. J. Phys*., 38, p. 1441.

Huppert, H.E. and Miles, J.W., 1969: “Lee waves in a stratified flow, Part 3: Semi-elliptical obstacle,” *J. Fluid Mech*., 35, pp. 357–374.

Jones, W.L., 1967: “Propagation of internal gravity waves in fluids with shear flow and rotation,” *J. Fluid Mech*., 30, pp. 481–496.

Klemp, J.B. and Lilly, K.K., 1978: “Numerical simulation of hydrostatic mountain waves,” *J. Atmos. Sci*., 35, pp. 78–107.

Lamb, 1932: *Hydrodynamics*, Cambridge University Press.

Landau, D.M. and Wurtele, M.G., 1991: “Resonant backscattering of a gravity wave from a critical level,” Eighth Conference on Atmospheric and Oceanic Waves and Stability, American Met. Soc., pp. 244–247.

Lilly, D.K., 1978: “A severe downslope windstorm and aircraft turbulence event induced by a mountain wave,” *J. Atmos. Sci*., 35, pp. 59–77.

Lindzen, R.S., 1981: “Turbulence and stress owing to gravity wave and tidal breakdown,” *J. Geophys. Res*., 86, pp. 9707–9714.

Lipps, F.B. and Hemler, R.S., 1982: “A scale analysis of deep moist convection and some related numerical considerations,” *J. Atmos. Sci*., 39, pp. 2192–2210.

Long, R.R., 1955: “Some aspects of the flow of stratified fluids,” *Tellus*, 7, pp. 341–357.

Lyra, G., 1943: “Theorie der stationaren leewellwenstromung in freier atmosphare,” *Z. angew. Math. Mech*., 23, pp. 1–28.

Ogura, Y. and Phillips, N.A., 1962: “Scale analysis of deep and shallow convection in the atmosphere,” *J. Atmos. Sci*., 40, pp. 396–427.

Palm, E. and Foldvik, A., 1960: “Contribution to the theory of two-dimensional mountain waves,” *Geofys. Publik*., 20:3, pp. 1–25.

Peltier, W.R. and Clark, T.L., 1983: “Nonlinear mountain waves in two and three spatial dimensions,” *Quart. J. Roy. Met. Soc*., 109:461, pp. 527–548.

Queney, P., 1948: “The problem of airflow over mountains: A summary of theoretical studies.” *Bull. Amer. Meteor. Soc*., 29, pp. 16–26.

Rottger, J. and Larsen, M.F., 1990: “UHF/VHF radar techniques for atmospheric research and wind profiler applications,” in *Radar in Meteorology*, American Met. Soc. (publisher), D. Atlas (ed.), pp. 235–281.

Scorer, R.S., 1949: “Theory of waves in lee of mountains,” *Quart. J. Roy. Met. Soc*., 75, pp. 41–56.

Sharman, R.D., and Wurtele, M.G., 1983: “Ship waves and lee waves,” J. *Atmos. Sci*., 40, pp. 396–427.

Sharman, R.D., Keller, T.L., and Wurtele, M.G., 1988: “Incompressible and anelastic flow simulations on numerically generated grids,” *Mon. Wea. Rev.*, 116, pp. 1124–1136.

Smith, S.A., Fritts, D.C., and VanZandt, D.T., 1987: “Evidence for a saturated spectrum of atmospheric gravity waves,” *J. Atmos. Sci*., 44:10, pp. 1404–1410.

Tanaka, H. and Yamanaka, M.D., 1984: “Propagation and breakdown of internal inertio-gravity waves near critical levels in the middle atmosphere,” *J. Met. Soc. Japan*, 62, pp. 1–17.

Wilhelmson, R., and Ogura, Y., 1972: “The pressure perturbation and the numerical modeling of a cloud,” *J. Atmos. Sci*., 29, pp. 1295–1307.

Wurtele, M.G., 1957: “The three dimensional lee wave,” *Beitr. Phys. Freien Atmos*., 29, pp. 242–252.

Wurtele, M.G., Sharman, R.D., and Keller, T.L., 1987: “Analysis and simulations of a tropospheric-stratospheric gravity wave model, Part I,” *J. Atmos. Sci*., 44, pp. 3269–3281.

Wurtele, M. G., Datta, A., and Sharman, R.D., 1991: “Propagation of resonant gravity-inertial waves,” Eighth Conference on Atmospheric and Oceanic Waves and Stability, American Met. Soc., pp. 364–367.

Yeh, K.C., and Liu, C.H., 1972: *Theory of ionospheric waves*, Academic Press, 477 pp.

REPORT DOCUMENTATION PAGE

Form Approved
OMB No. 0704-0188

1. AGENCY USE ONLY (Leave blank)	2. REPORT DATE	3. REPORT TYPE AND DATES COVERED
	June 1993	Contractor Report

4. TITLE AND SUBTITLE

Lee Waves: Benign and Malignant

5. FUNDING NUMBERS

WU 505-68-50
NCC 2-0374

6. AUTHOR(S)

M.G. Wurtele, A. Datta, and R.D. Sharman

7. PERFORMING ORGANIZATION NAME(S) AND ADDRESS(ES)

Department of Atmospheric Sciences
University of California
Los Angeles, CA 90024-1565

8. PERFORMING ORGANIZATION REPORT NUMBER

H-1890

9. SPONSORING/MONITORING AGENCY NAME(S) AND ADDRESS(ES)

NASA Dryden Flight Research Facility
P.O. Box 273
Edwards, California 93523-0273

10. SPONSORING/MONITORING AGENCY REPORT NUMBER

NASA CR-186024

11. SUPPLEMENTARY NOTES

NASA technical monitors were K. Iliff and L.J. Ehernberger, Dryden Flight Research Facility.

12a. DISTRIBUTION/AVAILABILITY STATEMENT

Unclassified—Unlimited
Subject Category 47

12b. DISTRIBUTION CODE

13. ABSTRACT (Maximum 200 words)

The flow of an incompressible fluid over an obstacle will produce an oscillation in which buoyancy is the restoring force, called a gravity wave. For disturbances of this scale, the atmosphere may be treated as dynamically incompressible, even though there exists a mean static upward density gradient. Even in the linear approximation—i.e., for small disturbances—this model explains a great many of the flow phenomena observed in the lee of mountains. However, nonlinearities do arise importantly, in three ways: (i) through amplification due to the decrease of mean density with height; (ii) through the large (scaled) size of the obstacle, such as a mountain range; and (iii) from dynamically singular levels in the fluid field. These effects produce a complicated array of phenomena—large departure of the streamlines from their equilibrium levels, high winds, generation of small scales, turbulence, etc.—that present hazards to aircraft and to lee surface areas. The nonlinear disturbances also interact with the larger-scale flow in such a manner as to impact global weather forecasts and the climatological momentum balance. If there is no dynamic barrier, these waves can penetrate vertically into the middle atmosphere (30–100 km), where recent observations show them to be of a length scale that must involve the coriolis force in any modeling. At these altitudes, the amplitude of the waves is very large, and the phenomena associated with these wave dynamics are being studied with a view to their potential impact on high performance aircraft, including the projected National Aerospace Plane (NASP). The presentation herein will show the results of analysis and of state-of-the-art numerical simulations, validated where possible by observational data, and illustrated with photographs from nature.

14. SUBJECT TERMS

Clear air turbulence, Gravity waves, Inertia-gravity waves, Lee waves

15. NUMBER OF PAGES

30

16. PRICE CODE

AO3

17. SECURITY CLASSIFICATION OF REPORT	18. SECURITY CLASSIFICATION OF THIS PAGE	19. SECURITY CLASSIFICATION OF ABSTRACT	20. LIMITATION OF ABSTRACT
Unclassified	Unclassified	Unclassified	Unlimited